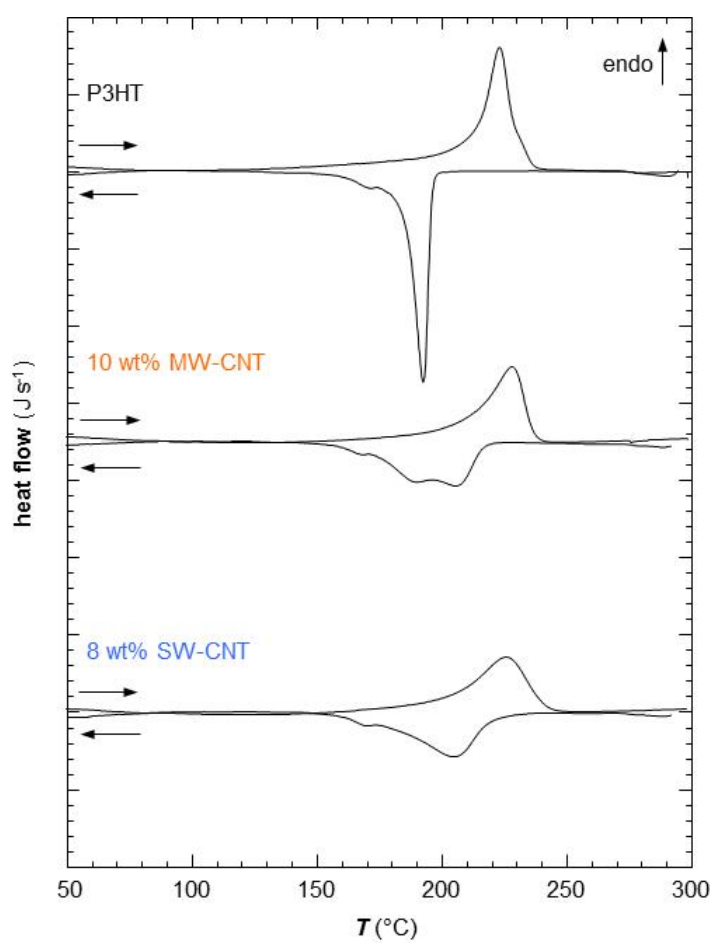


## Electronic Supplementary Information

# Thermoelectric composites of poly(3-hexylthiophene) and carbon nanotubes with a large power factor

Celine Bounioux, Pablo Díaz-Chao, Mariano Campoy-Quiles, Marisol S. Martín-González,  
Alejandro R. Goñi, Rachel Yerushalmi-Rozen and Christian Müller



**Fig. S1** Differential scanning calorimetry (DSC) second heating and cooling thermograms of P3HT and composites with  $c_{\text{MW-CNT}} \sim 10 \text{ wt\%}$  and  $c_{\text{SW-CNT}} \sim 8 \text{ wt\%}$ .

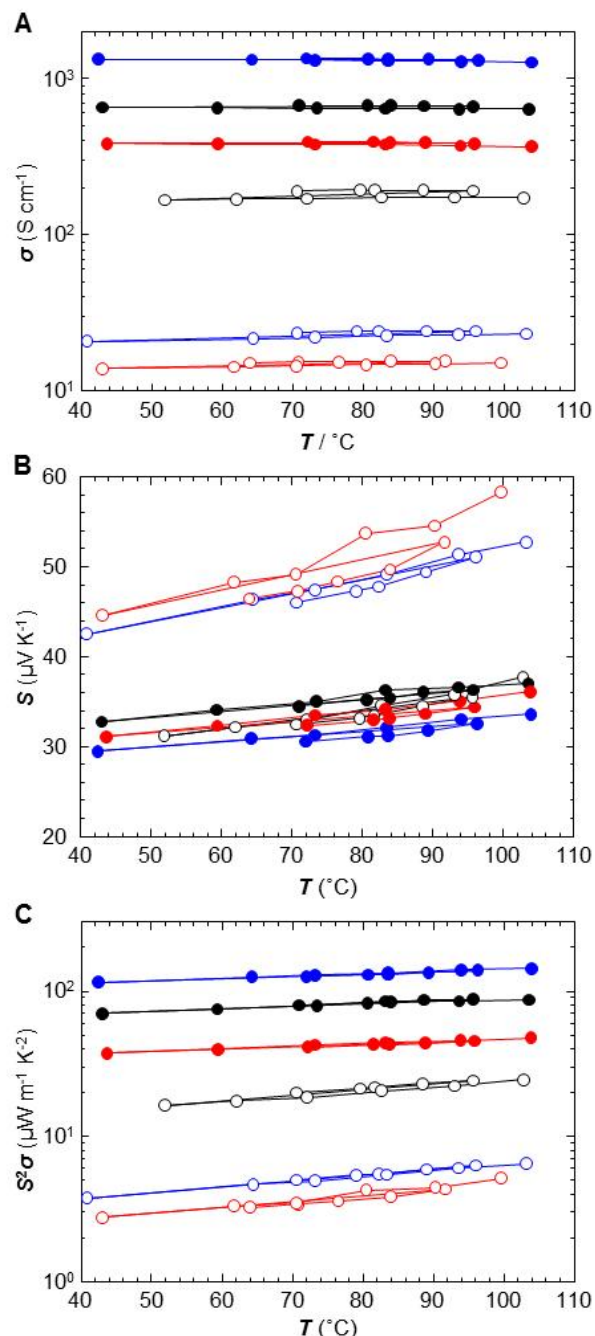


**Fig. S2** Temperature-dependent electrical properties cycled twice between 40–105 °C of two P3HT/SW-CNT composites with composition  $c_{\text{SW-CNT}} \sim 42$  wt% (blue and red) and  $c_{\text{SW-CNT}} \sim 81$  wt% (black), as-cast (open circles) and doped (filled circles). (A) electrical conductivity  $\sigma$ ; (B) the Seebeck coefficient  $S$  and (C) the power factor  $S^2\sigma$ . The data for 42 wt% SW-CNT were measured for two independently prepared samples and differences are likely due to different degrees of dispersion of SW-CNTs.

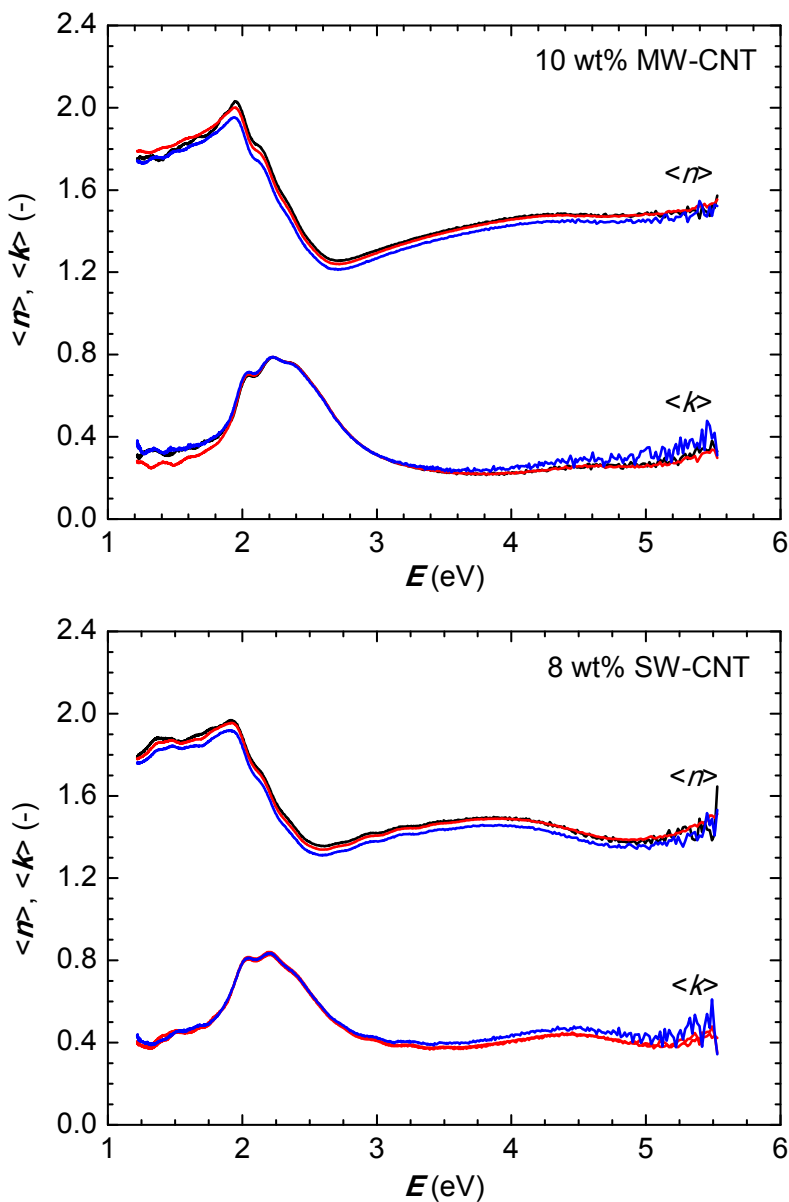


**Fig. S3** Pseudo refractive index  $\langle n \rangle$  and extinction coefficient  $\langle k \rangle$  of 10wt% MW-CNT and 8 wt% SW-CNT composites obtained by direct analytical inversion of the ellipsometric angles measured at an incidence angle of 50° (black), 60° (red) and 70° (blue) assuming an isotropic and optically infinite medium. The apparent invariance of the pseudo optical constants with the incidence angle strongly suggests that these samples are largely isotropic.

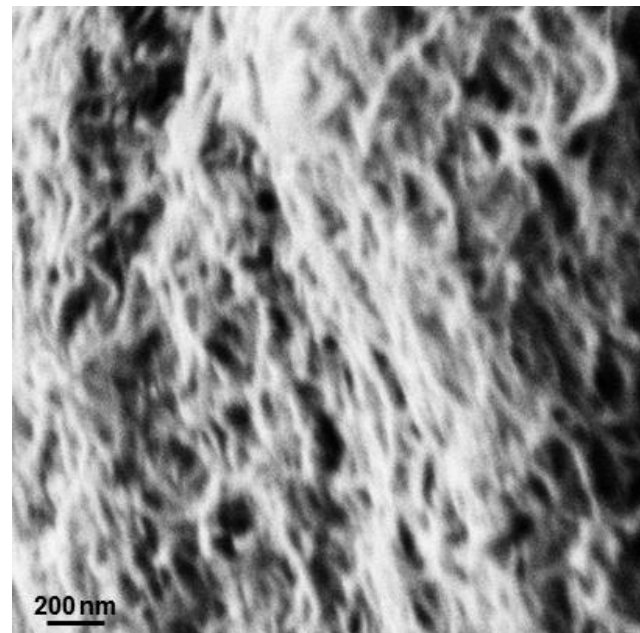


**Fig. S4** Scanning electron micrograph of a P3HT/MW-CNT composite with  $c_{\text{MW-CNT}} \sim 50 \text{ wt\%}$ .

The image was recorded with a Leo Ultra 55 FEG instrument.

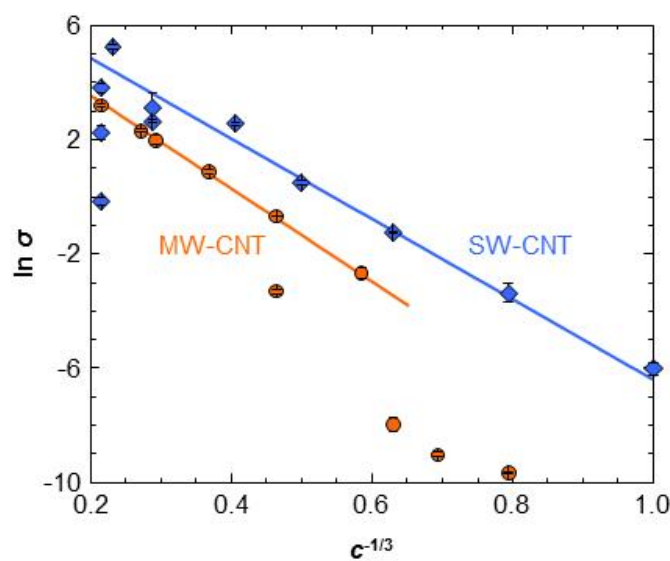


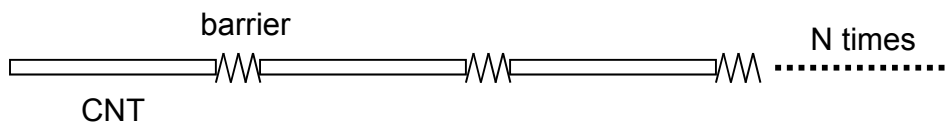
**Fig. S5** Plot of  $\ln \sigma$  vs.  $c^{-1/3}$  of undoped samples. The good linear fit above the percolation threshold indicates that tunnel junctions limit electrical transport. For fitting, we excluded low MW-CNT compositions  $c \leq 4 \text{ wt\%}$  as well as reference SW-CNT.

## General description of conductance in polymer/CNT composites

In polymer/CNT composites there are two possible conductance channels in parallel, one is the polymer matrix and the other one is the CNT network joint together via polymer barriers. The conductance of such a composite is given by:

$$G_{total} = (1 - c) \cdot G_{polymer} + c \cdot G_{network}$$

where  $c$  is the concentration of CNTs. The CNT network is composed of CNTs that are connected in series via polymer barriers:



Thus, the conductance  $G_{network}$  of the CNT plus barrier system is given by:

$$\frac{1}{G_{network}} = \frac{1}{G_{CNT}} + \frac{1}{G_{barrier}} + \frac{1}{G_{CNT}} + \frac{1}{G_{barrier}} + \dots = N \left( \frac{1}{G_{CNT}} + \frac{1}{G_{barrier}} \right).$$

When considering that the barrier has a much lower conductance than the CNTs, *i.e.*  $G_{CNT} \gg G_{barrier}$ , we obtain:

$$G_{network} \sim \frac{1}{N} \cdot G_{barrier}.$$

For the whole composite film we obtain:

$$G_{total} \sim (1 - c) \cdot G_{polymer} + \frac{c}{N} \cdot G_{barrier}.$$

Below the percolation threshold of CNTs,  $G_{barrier} \leq G_{polymer}$  and thus:

$$G_{Total} \sim (1 - c - \frac{c}{N}) \cdot G_{polymer} \sim G_{polymer}$$

since  $c$  and  $c/N$  are small in this regime. This is indeed what we observe experimentally for the electrical and thermal conductivity of undoped as well as doped P3HT/CNT composites.

On the other hand, above the percolation threshold the conductance of the polymer channel is much lower than the conductance of the network, *i.e.*  $G_{polymer} \ll G_{network}$ , and thus:

$$G_{Total} \sim \frac{c}{N} \cdot G_{barrier} \propto c.$$

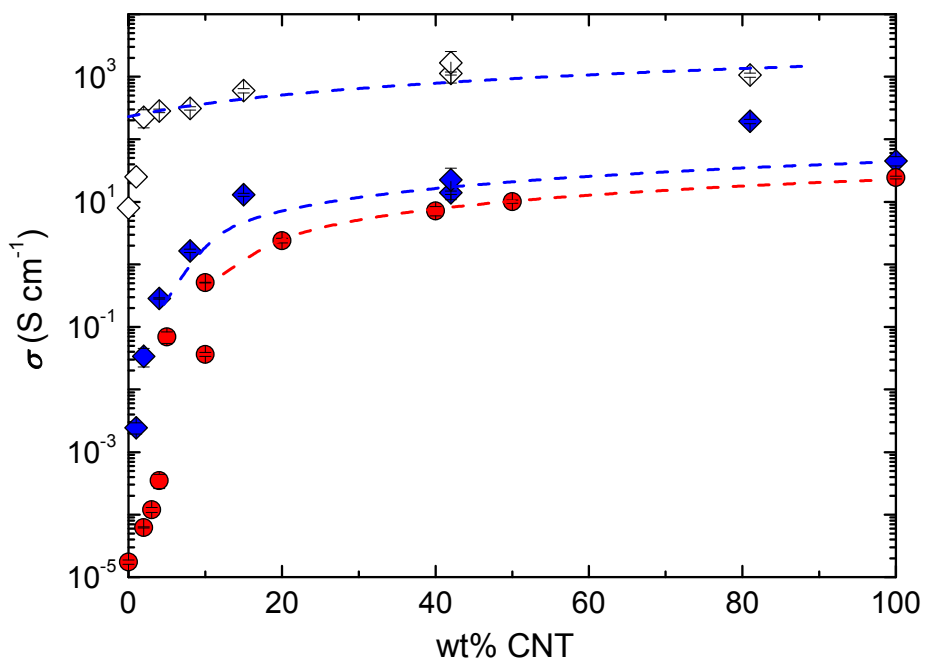


**Fig. S6** At compositions above the percolation threshold,  $\sigma \propto c$  provides a good fit to undoped P3HT/MW-CNT (red circles) and P3HT/SW-CNT composites (blue diamonds) as well as doped P3HT/SW-CNT composites (open diamonds). For doped MW-CNT composites, our approximation  $G_{\text{polymer}} \ll G_{\text{network}}$  is not valid since in this case  $\sigma_{\text{P3HT}} \sim \sigma_{\text{MW-CNT}}$ .

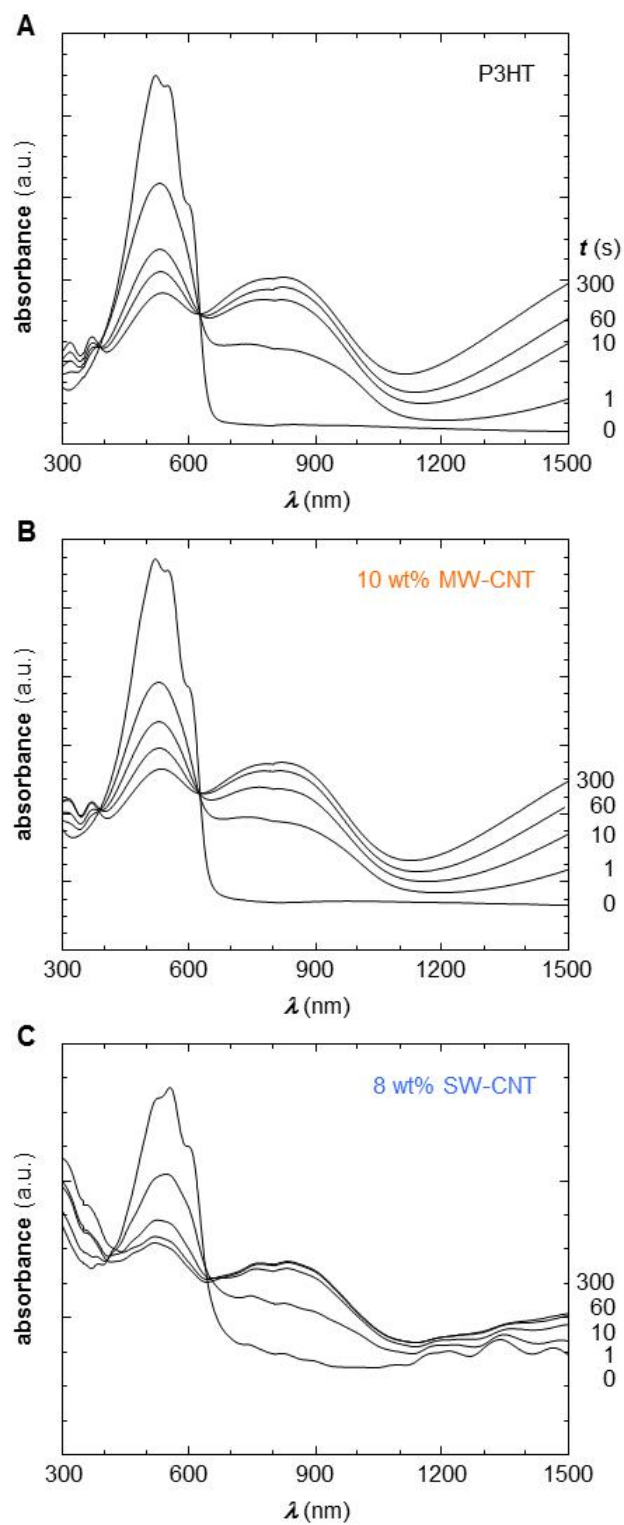


**Fig. S7** UV-vis absorbance spectra for different doping times of spin-coated thin films of (A) regioregular P3HT; (B) a composite with  $c_{\text{MW-CNT}} \sim 10 \text{ wt\%}$ ; and (C) a composite with  $c_{\text{SW-CNT}} \sim 8 \text{ wt\%}$ .

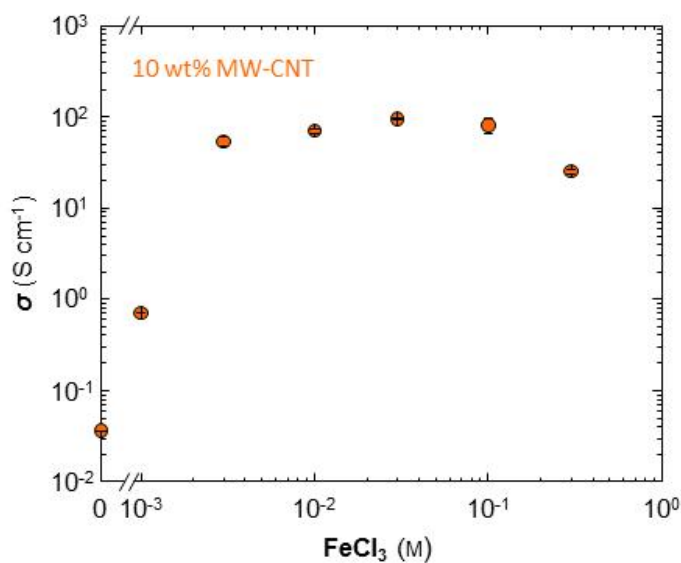


**Fig. S8**  $\sigma$  of a composite with  $c_{\text{MW-CNT}} \sim 10$  wt% doped for one hour with various concentrations of anhydrous  $\text{FeCl}_3$  in nitromethane. The apparent decrease for strongly doped samples is likely due to the significant increase in brittleness.

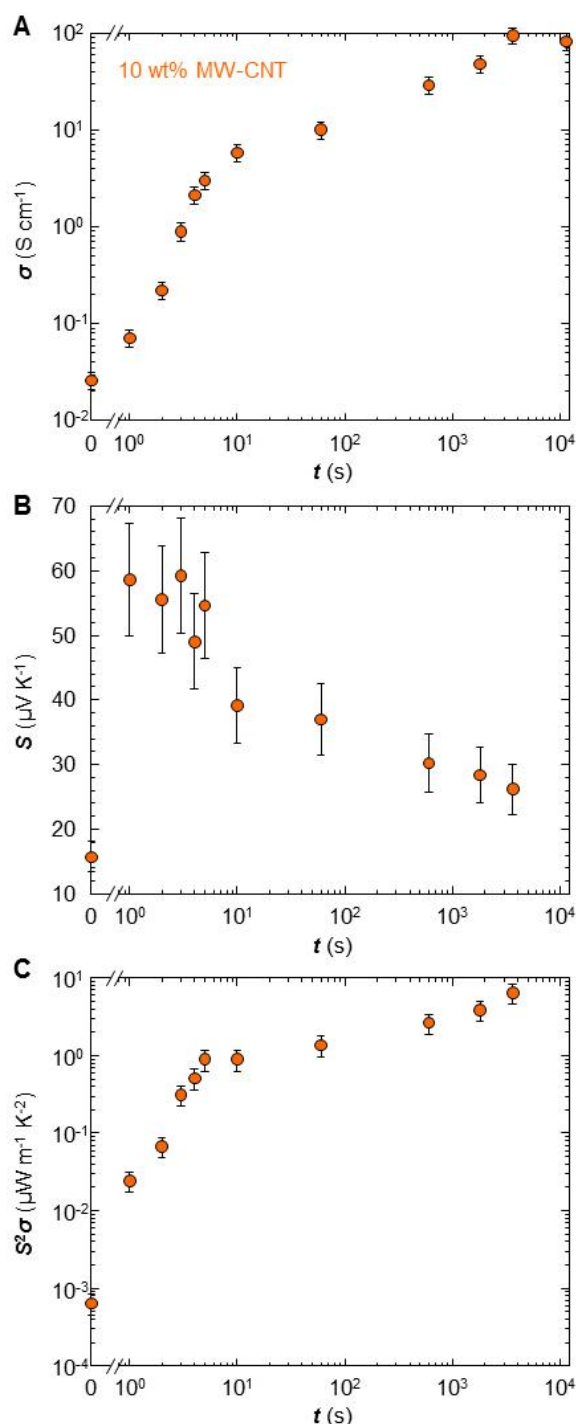


**Fig. S9** (A)  $\sigma$ , (B)  $S$  and (C)  $S^2\sigma$  of a composite with  $c_{\text{MW-CNT}} \sim 10$  wt% as a function of doping time; doping with 0.03 M anhydrous  $\text{FeCl}_3$  in nitromethane. The electrical conductivity  $\sigma$  continuously increases up to  $t = 3600$  s but decreases for larger doping times. The Seebeck coefficient  $S$  displays a maximum at intermediate doping time  $t \sim 1-5$  s. Note that we did not measure the Seebeck coefficient for  $t > 3600$  s.

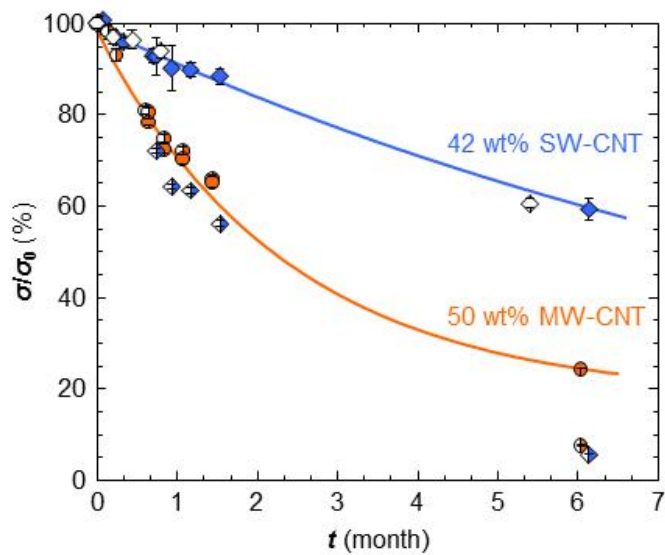


**Fig. S10** Ratio  $\sigma/\sigma_0$  of remaining  $\sigma$  time  $t$  after doping and initial  $\sigma_0$  directly after doping for one hour in 0.03 M anhydrous  $\text{FeCl}_3$  in nitromethane. Samples were stored at ambient. Compositions:  $c_{\text{MW-CNT}} \sim 10 \text{ wt\%}$  (half-filled circles),  $c_{\text{MW-CNT}} \sim 50 \text{ wt\%}$  (filled circles),  $c_{\text{SW-CNT}} \sim 8 \text{ wt\%}$  (half-filled diamonds),  $c_{\text{SW-CNT}} \sim 42 \text{ wt\%}$  (filled and open diamonds). Solid lines are exponential fits.

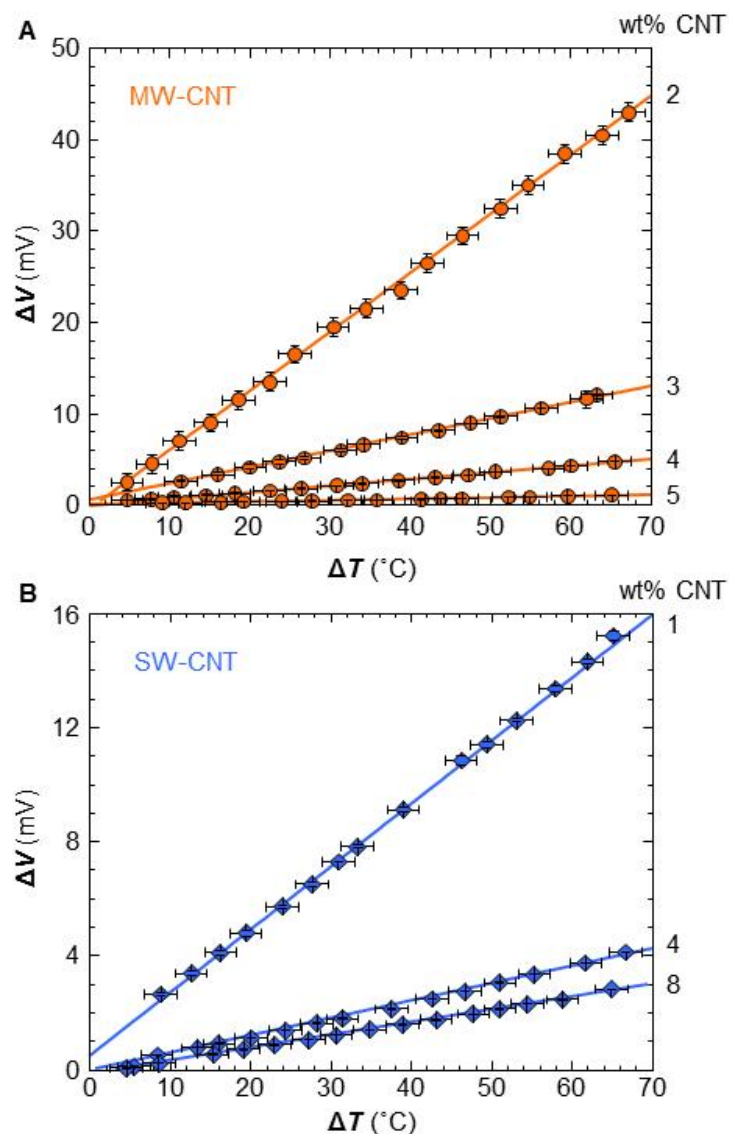


**Fig. S11** Potential difference  $\Delta V$  measured across (A) low-concentration P3HT/MW-CNT and (B) P3HT/SW-CNT tapes as a function of experienced temperature difference  $\Delta T$  between the two ends of each tape. Average relative Seebeck coefficients  $\Delta S$  were estimated from the slope of straight line fits.